EJN European Journal of Neuroscience

FENS Federation of European Neuroscience Societies

European Journal of Neuroscience, Vol. 40, pp. 3316–3327, 2014 doi:10.1111/ejn.12698

BEHAVIORAL NEUROSCIENCE

Neurons in the pigeon nidopallium caudolaterale signal the selection and execution of perceptual decisions

Daniel Lengersdorf,[1] Roland Pusch,[1] Onur Güntürkün[1] and Maik C. Stüttgen[1,2,3]

[1]Department of Biopsychology, Faculty of Psychology, University of Bochum, Bochum, Germany

[2]Institute of Pathophysiology, University Medical Center, Johannes Gutenberg University, Hanns-Dieter-Hüsch-Weg 19, 55128 Mainz, Germany

[3]Focus Program Translational Neuroscience, University Medical Center, Johannes Gutenberg University, Hanns-Dieter-Hüsch-Weg 19, 55128 Mainz, Germany

Keywords: bird, choice, decision making, psychophysics, reward

Abstract

Sensory systems provide organisms with information on the current status of the environment, thus enabling adaptive behavior. The neural mechanisms by which sensory information is exploited for action selection are typically studied with mammalian subjects performing perceptual decision-making tasks, and most of what is known about these mechanisms at the single-neuron level is derived from cortical recordings in behaving monkeys. To explore the generality of neural mechanisms underlying perceptual decision making across species, we recorded single-neuron activity in the pigeon nidopallium caudolaterale (NCL), a non-laminated associative forebrain structure thought to be functionally equivalent to mammalian prefrontal cortex, while subjects performed a visual categorisation task. We found that, whereas the majority of NCL neurons unspecifically upregulated or downregulated activity during stimulus presentation, ~20% of neurons exhibited differential activity for the sample stimuli and predicted upcoming choices. Moreover, neural activity in these neurons was ramping up during stimulus presentation and remained elevated until a choice was initiated, a response pattern similar to that found in monkey prefrontal and parietal cortices in saccadic choice tasks. In addition, many NCL neurons coded for movement direction during choice execution and differentiated between choice outcomes (reward and punishment). Taken together, our results implicate the NCL in the selection and execution of operant responses, an interpretation resonating well with the results of previous lesion studies. The resemblance of the response patterns of NCL neurons to those observed in mammalian cortex suggests that, despite differing neural architectures, mechanisms for perceptual decision making are similar across classes of vertebrates.

Introduction

Sensory systems provide organisms with information on the current status of environmental variables to enable adaptive behavior. In laboratory settings, the process by which sensory information is harnessed to decide on a course of action (perceptual decision making) is studied employing psychophysical tasks. Importantly, perceptual decision making entails not only sensory processing, but also taps non-sensory factors such as motivation (Stüttgen *et al.*, 2011a). Signal detection theory (Green & Swets, 1988) and sequential analysis (Gold & Shadlen, 2002) provide quantitative descriptions of the processes underlying the formation of perceptual decisions and can be extended to include the influence of non-sensory factors such as response bias and reinforcement contingency (Boneau & Cole, 1967; Alsop, 1998; Stüttgen *et al.*, 2011b, 2013). Accordingly, neural correlates of perceptual decisions are found not only in sensory areas but also in associative and premotor structures such as the parietal and frontal cortices (Kim & Shadlen, 1999; Shadlen & Newsome, 2001; Feierstein *et al.*, 2006).

Although the avian brain is devoid of a laminated cortex, comparative anatomical research in the past decades has revealed that the pallium, which comprises most of the avian telencephalon, is homologous to the mammalian cortex (Reiner *et al.*, 2005). Moreover, some pallial structures seem to support cognitive abilities that are on a par with those of mammals (Striedter, 2013). In particular, the nidopallium caudolaterale (NCL) constitutes an associative forebrain structure that is thought to be functionally analogous to the mammalian prefrontal cortex (PFC). Similar to the PFC, the NCL receives projections from all secondary sensory areas, is innervated by dopaminergic midbrain neurons, and directs its output to premotor structures (Güntürkün, 2005). Similar to the effects of damage to the PFC, lesions of the NCL impair performance in delayed alternation (Mogensen & Divac, 1982, 1993), go/no-go (Güntürkün, 1997), and working memory (Diekamp *et al.*, 2002a) tasks, and these effects cannot simply be ascribed to visual discrimination deficits (Mogensen & Divac, 1982, 1993; Hartmann & Güntürkün, 1998) or impaired visuomotor performance (Helduser & Güntürkün, 2012).

Correspondence: Maik C. Stüttgen, [2]Institute of Pathophysiology and [3]Focus Program Translational Neuroscience, University Medical Center, as above.
E-mail: maik.stuettgen@uni-mainz.de

Received 11 April 2014, revised 24 June 2014, accepted 17 July 2014

Furthermore, single-neuron recording studies have revealed that NCL neurons respond to conditioned stimuli predicting reward (Kalt *et al.*, 1999; Kirsch *et al.*, 2009) and fire during the delay phase in working memory tasks (Diekamp *et al.*, 2002b; Browning *et al.*, 2011), resembling PFC response patterns (Fuster, 1973; Thorpe *et al.*, 1983).

In view of these findings, we hypothesised that the NCL participates in the translation of sensory information to goal-directed behavior, as is required for perceptual decisions. We subjected pigeons to a psychophysical single-interval forced-choice task resembling paradigms previously employed with monkeys (Newsome *et al.*, 1989; De Lafuente & Romo, 2005) and rats (Krupa *et al.*, 2001; Brunton *et al.*, 2013; Zariwala *et al.*, 2013) to examine the role of the NCL in perceptual decision making. The similarity of the psychophysical tasks allowed us to compare neural responses in the NCL with those observed in the mammalian cortex to examine the degree to which neural correlates of decision making are shared by different classes of vertebrates.

Materials and methods

Subjects

Eight homing pigeons (*Columba livia forma domestica*) served as experimental subjects. The birds were obtained from local breeders, raised in the institute's own aviary, and housed individually in wire-mesh cages inside a colony room (12 h light/dark cycle, lights off at 20:00 h). Water was available *ad libitum*. On workdays, access to food was restricted to testing periods in the experimental chamber; on weekends, food was available in the home cages. Pigeons were maintained close to 85% of their free-feeding weight. Subjects were treated according to the German guidelines for the care and use of animals in science, and all procedures were approved by a national ethics committee of the State of North Rhine–Westphalia, Germany and were in accordance with the European Communities Council Directive 86/609/EEC regarding the care and use of animals for experimental procedures.

Apparatus and procedure

Testing was conducted in an operant chamber measuring 34 × 34 × 50 cm. The back wall of the chamber featured three horizontally arranged rectangular translucent response keys (4 × 4 cm, bottom height from the floor 17 cm) coupled to electric switches. An LCD flat screen, mounted against the back wall of the chamber, was used for stimulus presentation. Effective key pecks produced feedback clicks. Grain food could be delivered through a food hopper located below the center key. The experimental chamber was positioned in a sound-attenuating cubicle. White noise (approximately 80 dB) was constantly present. The hardware was controlled by custom-written Matlab code (The Mathworks, Natick, MA, USA) (Rose *et al.*, 2008).

Pigeons performed a single-interval forced-choice task which is sketched in Fig. 1A. Sample stimuli were six uniform gray rectangles that were visible through the center key. The grayscale values employed were 130, 150, 170, 190, 210, and 230 [the display's range extended from 0 to 255; the category boundary (180) roughly corresponded to an illuminance of 54 lux; see six squares on the right of the panel]. Three stimuli with grayscale values < 180 were assigned to category C1 or 'dark', and three stimuli with grayscale values > 180 were assigned to category C2 or 'bright'. After an intertrial interval (ITI) of 3 s, the center key was illuminated green. If the animal initialised the trial by pecking once within 5 s, one of the six sample stimuli was presented for 1 s on the same key. Immediately after sample stimulus offset, the center key was again transilluminated green. Another single key peck turned off the center key and activated the side (choice) keys (also transilluminated green). The animals' task was to respond to the right choice key after one of the three dark (C1) stimuli had been presented, and to respond to the left choice key after one of the three bright (C2) stimuli had been presented. Following a correct response, food was delivered on a fraction of trials (ranging from 0.4 to 0.8 across sessions) after a delay of 1, 2, or 3 s (occurring with a probability of 0.5, 0.33, and 0.17, respectively). The food hopper was illuminated from the start of the delay period to the end of the 1.75 s food presentation. On the remaining fraction of trials, the

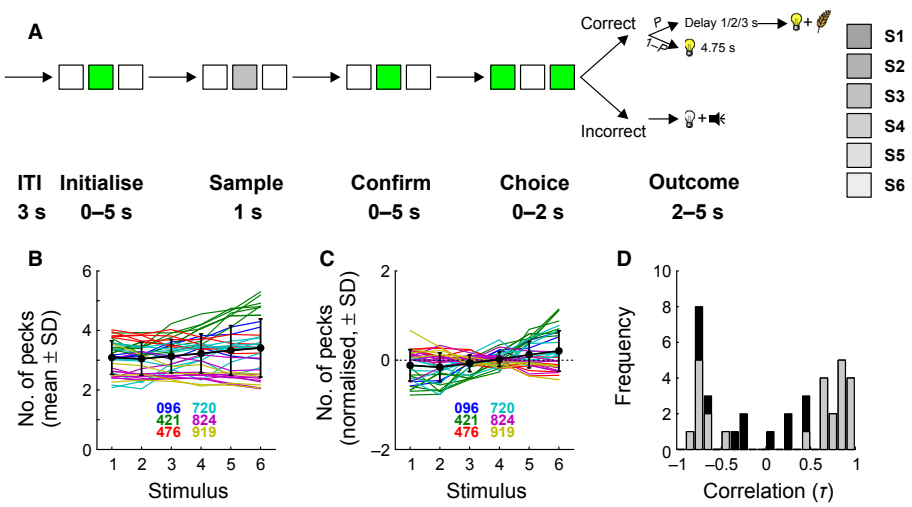

FIG. 1. Behavioral results. (A) Schematic outline of the behavioral task. Horizontally arranged squares represent the three response keys. Time ranges denote the minimum and maximum duration of each phase of the task. The trial was aborted if the animal did not respond before the maximum duration of a task elapsed. The six vertically arranged squares on the right show the grayscale stimuli that the pigeons had to categorise. See Materials and methods for further details. (B) Mean number of key pecks during the sample phase as a function of stimulus identity, plotted separately for the six different subjects (color-coded). Bold black lines indicate means and SDs across all birds and sessions. (C) As in (B), but normalised by subtracting the mean response level in each session. (D) Kendall's τ correlation between the number of key pecks emitted to a certain stimulus and the identity of that stimulus (coded as ordinal values from 1 to 6). Black bars, all sessions; gray bars, sessions with statistically significant τ values only.

food hopper was illuminated for 4.75 s without accompanying food hopper activation ('food omission'). Following an incorrect response, houselights were turned off for 2 s ('punishment'). In most sessions (for 66 out of 75 units), food was occasionally presented between two ITIs without any response requirement (henceforth dubbed 'free food'). Presentation of free food occurred, on average, after every 24th trial (i.e. 25 times per session of 600 trials).

Surgery

After reaching asymptotic task performance, six animals were implanted with custom-built microdrives. Pigeons were anesthetised with isoflurane supplemented by an injection of butorphanol (3 mg in 3 ml solution), and placed in a stereotaxic apparatus. The skin overlying the skull was incised and pulled sideways. Stainless steel microscrews were placed on the skull to anchor the dental cement head mount. One screw served as ground for electrophysiological recordings. A small trepanation was made in the skull overlying the left or right NCL. Electrodes were targeted to the coordinates AP –5.5, ML ±7.0 mm and implanted just below the brain surface. The microdrive was fastened to the skull with dental cement. Animals received an injection of analgesics (Carprofen, 10 mg/kg) for 3 days following surgery and were allowed to recover for a minimum of 2 weeks before testing.

Electrophysiology

The materials and recording procedures have been described in detail elsewhere (Starosta *et al.*, 2013, 2014). Briefly, neural signals were picked up by eight formvar-insulated nichrome wires (25 μm o.d., impedance ~0.5 MΩ) (Stablohm 675, California Fine Wire, Grover Beach, USA) connected to microplugs (Ginder Scientific, Nepean, CA, USA) housed in a custom-built microdrive implant (Bilkey & Muir, 1999; Bilkey *et al.*, 2003), passed through a custom-built headstage with unity gain, amplified 1000 × and bandpass-filtered from 0.5 to 5 kHz online by a difference amplifier (DPA-2FS, npi electronic GmbH, Germany), and digitised using an analog-to-digital converter (power 1401, Cambridge Electronic Design, Cambridge, UK) with sampling rates of 16–20 kHz. The raw data were stored with Spike2 Version 7 (Cambridge Electronic Design). All channels were digitally bandpass-filtered from 0.5 to 5 kHz. Spikes were extracted by amplitude thresholds and sorted manually in Spike2 using principal component analysis in combination with custom-written Matlab code. The signal-to-noise-ratio was computed as the peak-to-peak amplitude of the average waveform, divided by the trimmed width of the noise band (distance between the 2.5th and 97.5th percentile of noise amplitude values). By that criterion, the signal-to-noise-ratios of our units ranged from 1.4 to 5.7 (median, 2.3). Assuming normal distributions, this corresponded to 5.6–22.8 SDs distance of maxima and minima. None of the 75 units that entered the final data set displayed interspike intervals of less than 1 ms. Particular care was taken to identify and exclude artifacts resulting from key pecking (i) by inspecting raw waveform traces and (ii) by examining each unit's peri-peck time histogram (PPTH), i.e. a peri-stimulus time histogram triggered on individual key pecks, for conspicuous waveforms and peaks near time point 0.

Histology

After completion of the experiments, pigeons were deeply anaesthetised with Equithesin (4.5–5.5 mL/kg body weight) and perfused intracardially with 0.9% saline followed by 4% paraformaldehyde. Brains were removed, sectioned at 40 μm, and every fifth slice was stained with cresyl violet. The point of largest expansion of the cannula track was used to estimate the position of the recording sites along the anterior–posterior and mediolateral axes.

Data analysis

The spontaneous firing rate was calculated over the last 2 s of the ITI, i.e. the time before the initialisation stimulus appeared. Spike-density functions were constructed by convolving peri-stimulus time histograms of 1 ms temporal resolution with an exponentially modified Gaussian kernel with an SD of 100 ms and a time constant of 100 ms.

The spike count differences for two samples were expressed as the area under the receiver operating characteristic curve (AUROC). The AUROC reveals how much information a neuron contains about which of two conditions is actually presented to an ideal observer, who only knows the total spike count. A value of 0.5 signifies complete overlap of the two distributions, whereas values of 0 or 1 denote their complete separability. When more than two samples of spike counts were compared, we used η^2 as a measure of effect size (see Hentschke & Stüttgen, 2011). η^2 ranges from 0 to 1 and denotes the fraction of the total variance that is explained by the variance of the means of the distributions, i.e. $\eta^2 = SS_{between}/SS_{total}$, where $SS_{between}$ represents the sum of squared deviations between groups and SS_{total} represents the overall sum of squares. Put simply, this effect size measure illustrates how much of the total variance is due to there being different groups. Here, we will designate its magnitude as 'small' for values < 0.1, 'moderate' for $0.1 < \eta^2 < 0.2$, and 'large' for values > 0.3 (also see Cohen, 1992).

To check for premotor activity, we compared spike counts in the time window from –130 to –65 ms with spike counts in the time window from –65 to 0 ms relative to the first key peck to the initialisation stimulus. These values were chosen because previous work has shown that the time interval from pecking key fixation until the beak contacts the key encompasses roughly 65 ms (Zeigler *et al.*, 1980; Goodale, 1983). Minor modifications of these time spans had little effect on the results.

To test for the motor-related modulation of firing rate during sample presentation, we constructed PPTHs, i.e. peri-stimulus time histograms triggered to all key pecks that occurred within 100–900 ms of the sample phase. We subdivided spike counts within ± 100 ms of each key peck into four bins of 50 ms each and used the non-parametric Chi-squared test to detect any upregulation or downregulation of firing rate in that time window (deviation from a uniform distribution). Key pecks occurring within 50 ms after previous pecks were excluded from the analysis as these were too fast to constitute genuine key pecks and instead may reflect either mechanical bouncing of the response key or successive upper and lower beak contacts (Blough, 1963; Jenkins & Moore, 1973; Goodale, 1983).

The extent to which neural responses during the sample phase predicted upcoming choices was quantified with a predictive index (PI) computed in an analogous manner to Shadlen & Newsome (2001). Spike counts during 250 ms epochs were compared for pairs of stimuli located equally far from the category boundary (i.e. S1 vs. S6, S2 vs. S5, and S3 vs. S4) using AUROC, and this analysis was repeated with sliding windows moved in steps of 50 ms. Only data from correct trials were used. The PI thus captured how well an ideal observer can predict the upcoming choice response on the basis of spike counts alone.

Because of the low firing rates of NCL neurons, spike count distributions were heavily skewed, advising against the use of parametric statistical procedures. Accordingly, spike count distributions were compared using the non-parametric Wilcoxon rank-sum test for two independent samples, the Wilcoxon signed-rank test for two dependent samples and the Kruskal–Wallis test for more than two samples. Behavioral data (key pecking) were analysed using the non-parametric Friedman test with η^2 as a measure of effect size. All analyses were conducted in MATLAB R2012A (The Mathworks).

Results

Behavior

We recorded 75 single neurons from six animals over 38 behavioral sessions. Of these, 49 and 26 neurons were located in the left and right hemispheres, respectively. On average, animals performed 459 trials per session (range 112–596). As animals were overtrained on the choice task before electrode implantation, performance during the recording sessions was high throughout (mean 84% correct responses, range 68–92%). Animals were mostly unbiased towards either choice key (mean 51% left responses, range 36–67%). Animals experienced an average of 184 food rewards per session (range 32–371), as well as 169 food omissions (range 42–326), and 67 punishments (range 22–122). During the 1 s of sample presentation, all animals pecked at the central response key in nearly all of the trials, despite the fact that key pecks during this phase were inconsequential. The number of key pecks directed onto the center key was, on average, very similar across stimuli, ranging from 3.0 to 3.3 key pecks ($P = 0.33$, Friedman test; $\eta^2 = 0.03$, bootstrapped 95% confidence interval 0.005–0.092, computed across all sessions and animals; Fig. 1B). However, inspection of behavior within individual sessions revealed that the pecking rate was indeed affected by stimulus identity; in 25 out of 37 sessions, pecking rates differed significantly across stimuli ($P < 0.05$, Kruskal–Wallis test). However, the absolute magnitude of these differences was rather moderate (median SD of normalised pecking rates, 0.22 pecks) (see Fig. 1C). Individual animals tended to exhibit a largely consistent bias for enhanced responding for either bright or dark stimuli [three birds preferred dark and three birds preferred bright, expressed as the τ correlation between stimulus number (1, darkest; 6, brightest) and the average number of key pecks] (see Fig. 1D).

Electrophysiology

In the following, we will present neural response patterns separately for each of the three phases of the behavioral task. For each phase, neural activity was first compared with baseline firing (estimated from sampling during the ITI); subsequently, neural responses were compared across different stimuli or events within a given task phase.

Sample phase

In the sample phase, animals were confronted with six different stimuli and had to form their decision whether to subsequently respond to the left or right choice key (cf. Fig. 1). A total of 60/75 neurons (80%) displayed overall changes in firing rate during this phase compared with baseline activity ($P < 0.05$, rank-sum test). Of these 60 neurons, the large majority (43) decreased firing. Figure 2A and B shows the spike-density functions of two example neurons with increased (Fig. 2A) and decreased (Fig. 2B) spiking activity during the sample phase (Fig. 2a1, a2, and b1, b2, respectively), along with their corresponding PPTHs (Fig. 2a3 and b3). The neuron in Fig. 2A displayed a clear modulation of firing rate relative

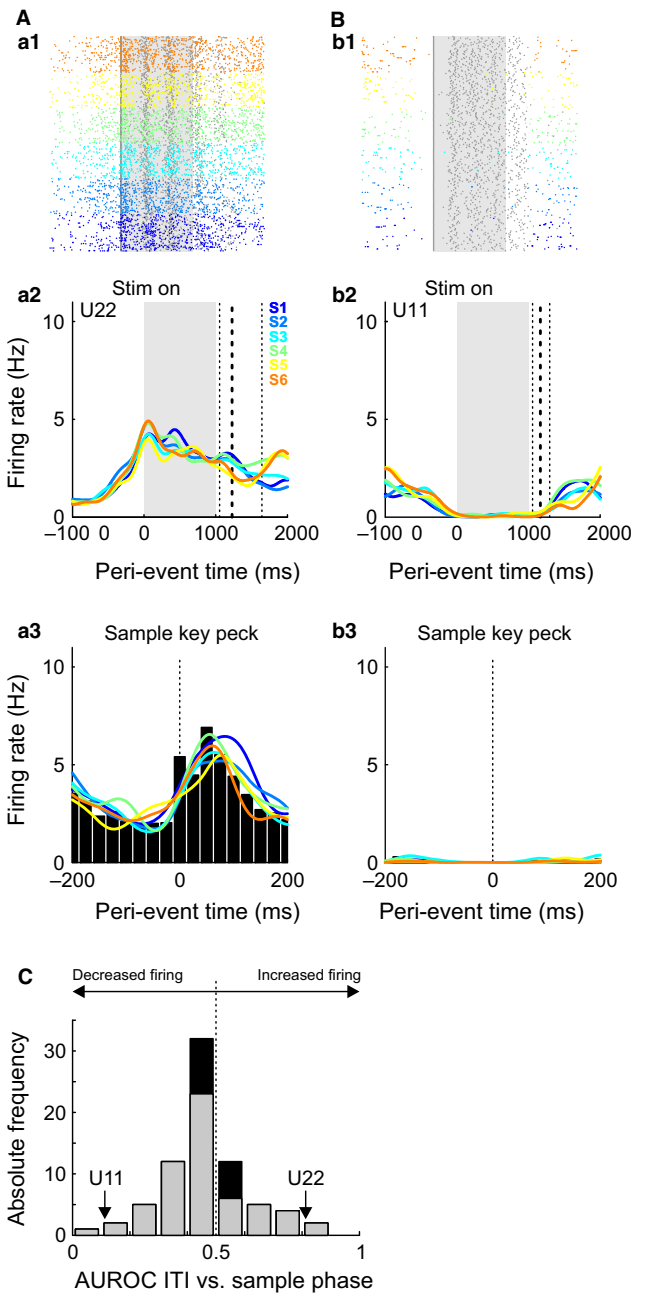

FIG. 2. Neural responses during the sample phase: comparison to baseline activity. (A) Example NCL neuron with significantly increased firing rate during the sample phase. (a1) raster display; (a2) spike-density functions (SDFs). Colors represent the six sample stimuli. Vertical dotted lines in (a2) indicate the 10th, 50th, and 90th percentiles of the distribution of leaving times, i.e. the time of the last peck to the center key, which terminated illumination and immediately preceded the beginning of the choice response to the left and right keys. Note that activity starts to increase over a few hundred milliseconds during the initialisation period, i.e. before the first key peck at stimulus onset. (a3) PPTH (black bars) depicting average firing rate during key pecking, along with trials split up according to the presently presented stimulus (colors) for the same neuron. SDFs were smoothed by an exponentially modified Gaussian kernel with $\tau = 100$ ms and $\sigma = 100$ ms. (B) As in (A), but for a neuron with significantly decreased firing rate during the sample phase. (C) Distribution of effect sizes (AUROC, see Materials and methods) for 74 NCL neurons. Black bars, effect sizes for all neurons; gray bars, statistically significant neurons only.

to key pecking, and firing rates were maximal at around 50 ms after the pigeon's beak hit the key; in contrast, the neuron in Fig. 2B was silent during key pecking. Neither neuron displayed differential activity for the six sample stimuli (colored lines). We quantified the degree of overall firing rate modulation (sample phase vs. ITI) using the AUROC (see Materials and methods). As is visible in Fig. 2C, there was a smooth distribution of effect sizes, indicating no obvious subdivision of modulated and non-modulated neurons.

In principle, such changes in firing rate could be brought about by (i) the animals' motor activity (recall that pigeons were key pecking throughout the sample phase) or (ii) presentation of the visual stimuli. To investigate to what extent NCL neurons showed motor-related activity, we conducted two separate analyses. First, we compared the firing rates during the 65 ms before the first key peck to the initialisation stimulus with the period from 130 to 65 ms before this event (because the forward thrust phase of a key peck lasts for about 65 ms) (Goodale, 1983). There were seven out of 74 neurons (9%) in which spike counts in the two time windows differed significantly (signed-rank test; for one neuron, center key pecks were not recorded), and all of them increased firing rates during the forward thrust. However, the magnitude of these spike count increases was generally small (most extreme AUROC value, 0.59).

Second, we examined the firing rates around pecks during the sample phase using the Chi-squared test (see Materials and methods). This analysis identified 20/74 (27%) neurons with motor-related firing rate modulation. This analysis is more sensitive than the previous one because it can detect modulations that do not result in a net change of firing rate. Only five of these 20 neurons displayed both a significant overall activity increase during the sample phase and significant modulation of the PPTH (an example is shown in Fig. 2A). In conclusion, more than half of the 56 neurons that showed significant increases or decreases in firing rate during the sample phase did not show response modulation associated with obvious aspects of motor activity and were thus presumably activated or deactivated by the presentation of the sample stimuli.

So far, we have only addressed the question of whether NCL neurons showed a general increase or decrease in firing during sample presentation, irrespective of stimulus identity. However, if the NCL were involved in decision formation or response selection, one would expect to find neurons whose firing rates differ across stimuli (henceforth dubbed 'stimulus-related modulation'). Indeed, we found that 15 of 75 neurons (20%) showed substantial stimulus-related modulations of firing rate ($P < 0.05$, Kruskal–Wallis test). Figure 3A and B shows two example neurons that fired differentially for the grayscale stimuli. Generally, differential activity emerged at about 100–300 ms after stimulus onset (Fig. 3a1, a2 and b1, b2). Importantly, the pace at which neural activity began to increase or decrease from baseline level was determined by the signed distance of the sample stimulus from the category boundary, being higher for easy stimuli of one particular response category (compare, e.g. S1 vs. S3 and S4 vs. S6). Moreover, when aligned to the confirmation response that immediately preceded choice execution (Fig. 3a3, a4 and b3, b4), it is evident that neural activity continued to differentiate the stimuli until the time of choice onset, which was on average 500 ms after the sample stimuli were turned off (cf. depiction of task flow in Fig. 1A and dashed vertical lines in Fig. 3a2 and b2). This stimulus-related modulation could not be attributed to the minor variations in pecking frequency (Fig. 1B and C), as neural activity continued to differentiate between the stimuli when aligned relative to individual key pecks (Fig. 3a6 and b6; $P < 0.05$, Kruskal–Wallis test).

Inspection revealed that all of the 15 neurons with significant stimulus-related modulations exhibited a pattern of nearly monotonically increasing or decreasing activity changes (in about equal proportions) with stimulus luminance. Importantly, most of these neurons (11/15) fulfilled the additional constraint that activity should significantly differ between stimuli when controlling for the rate of key pecking (as in Fig. 3a6 and b6). Thus, these neurons could, for example, code the brightness of the visual stimuli, or a motor plan for leftwards or rightwards movements after stimulus presentation. To separate sensory- and motor-related activity, we constructed spike-density functions separately for correct and error trials for the two stimuli closest to the category boundary for which the most error trials were recorded (> 10 trials per condition). For the neuron in Fig. 3a5, neural activity in correct S3 and incorrect S4 trials, as well as in correct S4 and incorrect S3 trials, was similar, demonstrating that firing reflected the animal's subsequent choice rather than the visual stimuli. This pattern was somewhat less clear for the neuron shown in Fig. 3b5. Nonetheless, averaging across all 11 neurons with sufficient numbers of error trials revealed that this subset of cells reflected the subsequently executed operant response rather than the brightness of the previously seen stimuli (Fig. 3C). Average firing rates in the 400 ms preceding confirmation were significantly different between correct and incorrect S3 trials, on the one hand, as well as correct and incorrect S4 trials, on the other hand (Wilcoxon signed-rank test, P-values < 0.05), signifying that identical stimuli (when followed by different behavioral responses) gave rise to different neural activity in correct and error trials. At the same time, neural activity did not differ significantly between correct S3 and incorrect S4 trials, as well as correct S4 and incorrect S3 trials (different stimuli followed by the same choice responses).

We quantified the degree to which neural responses predicted upcoming choices with a PI previously used by Shadlen & Newsome (2001). The PI denotes the probability that an ideal observer correctly predicts the upcoming leftwards or rightwards choice of the animal on the basis of a spike count comparison during a 250 ms epoch (see Materials and methods). Figure 4A–C shows the PI as a function of time, computed in steps of 50 ms and for three different pairs of stimuli. For both example cells (Fig. 4A and B, the same units as in Fig. 3A and B) as well as across the subset of modulated neurons (Fig. 4C), the PI increased more steeply for easy (S1 vs. S6) than for difficult (S3 vs. S4) discriminations and reached higher values toward the end of the stimulus period. To assess the statistical significance of this effect, we compared regression slopes for the PI values in the first 400 ms after stimulus onset. Regression slopes increased with decreasing stimulus difficulty [slopes for PI vs. time (s) were 0.095, 0.171 and 0.262 for S3 vs. S4, S2 vs. S5, and S1 vs. S6, respectively] and each slope was significantly different from the other two slopes (all P-values < 0.05, z-test).

The response pattern of these units resembled that of neurons recorded in macaque lateral intraparietal cortex and PFC in similar tasks (Kim & Shadlen, 1999; Shadlen & Newsome, 2001). These patterns are commonly interpreted to reflect the sensory evidence in favor of one of two distinct response categories (Gold & Shadlen, 2007). Importantly, the stimuli used in these studies (random-dot patterns in which only a fraction of dots moves coherently in one of two directions) differed from ours in an important respect, namely that subjects have to integrate motion information over time to form their decision; accordingly, performance improves with increasing stimulus presentation time. By contrast, our subjects were confronted with six different shades of gray whose luminance remained unchanged during the sample phase, so that, at least in principle, no integration of sensory evidence was necessary. In order to see

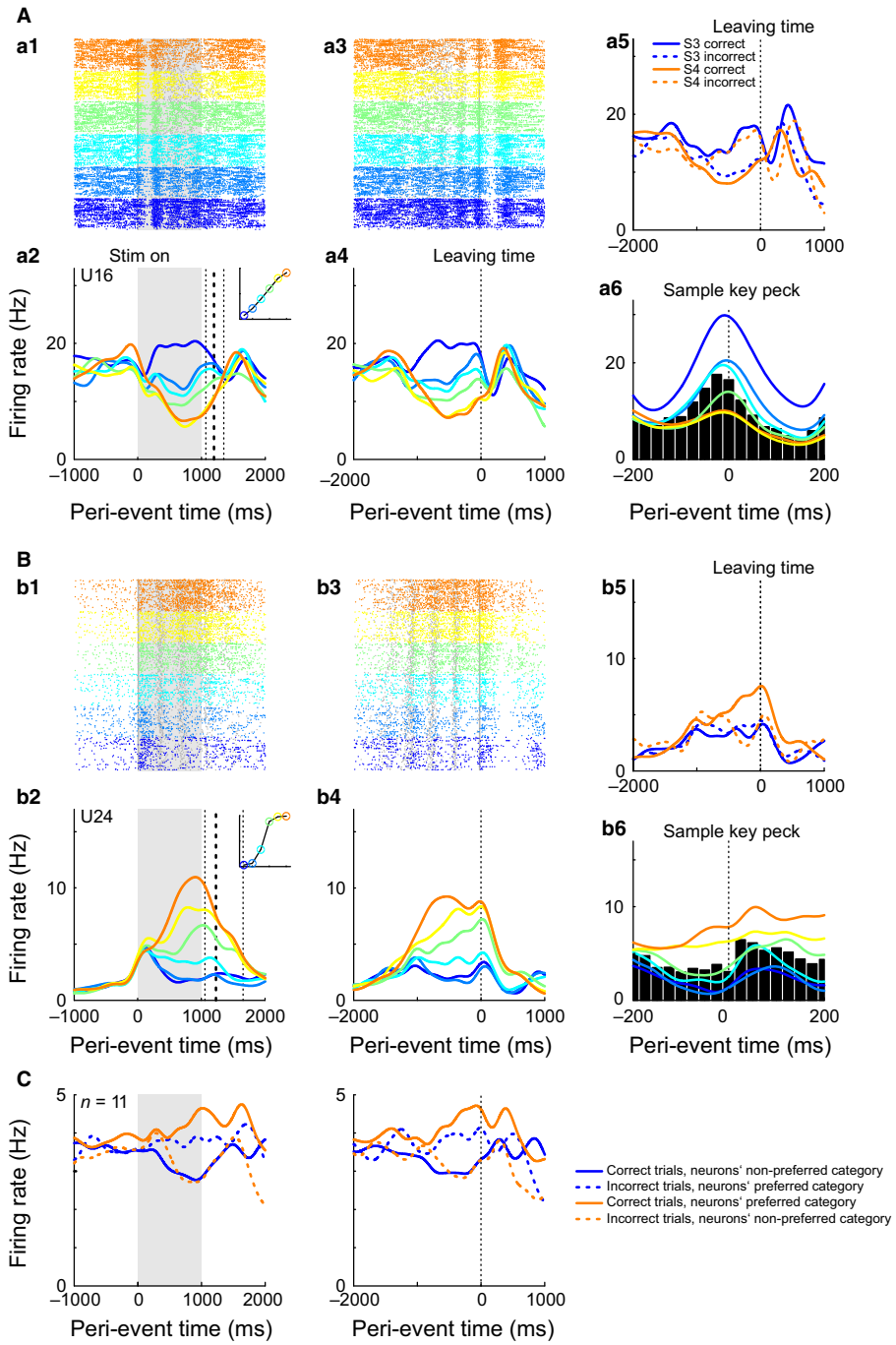

FIG. 3. Neural responses during the sample phase: within-phase differential modulation. (A) (a1 and a2) Example neuron with high baseline activity and differential activity during the sample phase [stimulus presentation highlighted by gray shaded background in (a2)]. Inset in (a2) shows psychometric curve obtained in the same session. (a3 and a4) The same data as in (a1) and (a2), but aligned to the confirmation response. (a5) Spike-density functions aligned to confirmation for stimuli S3 and S4 (enclosing the category boundary), split up according to whether the animal chose correctly or incorrectly. (a6) Corresponding PPTHs. Both the averaged (black bars) and individual (colors) PPTHs exhibited significant modulation. (B) As in (A), but for a neuron with low background activity. (C) As in (a5) and (b5), but aligned to either stimulus onset (left) or confirmation response (right) and averaged across all 11 neurons for which sufficient numbers of trials (≥10 per condition) were available. Because neurons preferred different response directions [cf. (A) and (B)], averages were not computed across stimuli but across preferred response directions, split up into correct and incorrect trials.

whether the psychophysical performance of subjects improved with increasing stimulus presentation times, we subjected two well-trained unimplanted animals to the same task as the other subjects, while additionally varying stimulus presentation times pseudorandomly within experimental sessions. As Fig. 4D shows, the psychophysical performance increased monotonically with stimulus presentation times from 0.1 to 1.0 s; this effect was highly significant for both birds (Chi-squared test; both P-values $< 10^{-75}$). Moreover, the time course of the performance increase (roughly 100–400 ms) resembled that of the PI (Fig. 3C). We concluded that our subjects did indeed integrate sensory information over time, even though the stimuli themselves were unchanging.

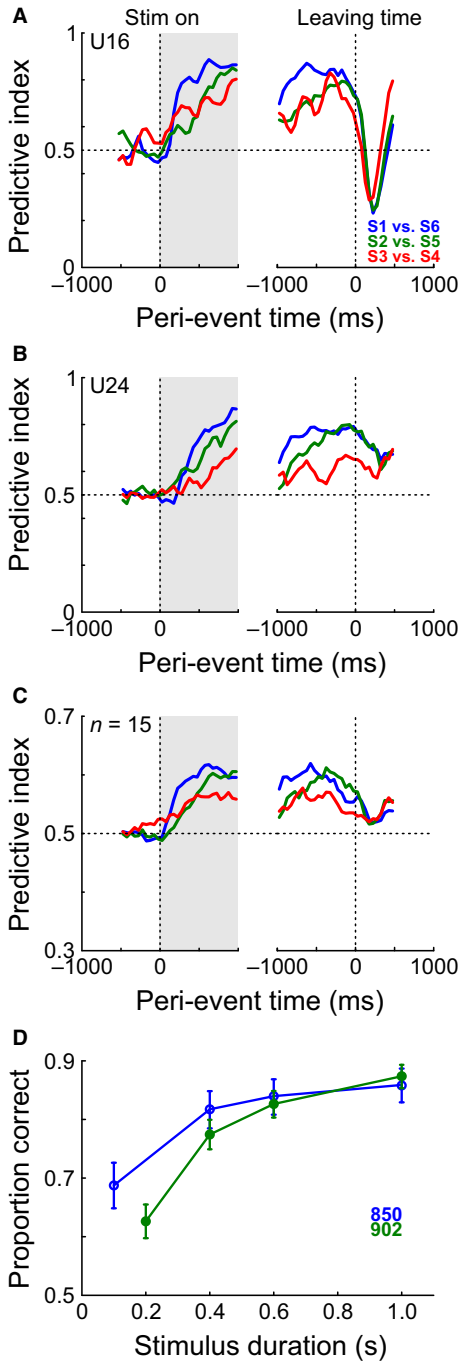

FIG. 4. Predictive power of neural responses during the sample phase. (A) PI (see Materials and methods) for three stimulus pairs during the sample phase, computed in sliding windows of 250 ms (moved in steps of 50 ms), for the unit shown in Fig. 3A. Values > 0.5 signify a tendency to respond into the neuron's preferred direction. Left panel: PI trajectories aligned to stimulus onset. Right panel: PI trajectories aligned to confirmation response. The analysis was conducted using correct trials only. (B) Same as in (A), but for the unit shown in Fig. 3B. (C) As in (A) and (B), but averaged across all neurons with significant within-phase differential modulation. Note the expanded ordinate relative to (A) and (B). (D) Psychophysical data (proportion correct responses across all stimuli) from two birds trained on the same task and confronted with four different stimulus presentation times. Error bars show binomial 95% confidence intervals.

To summarise, 80% of NCL neurons changed firing rate during the sample phase when the animal had to form its decision. The majority of neurons (46/75, 61%) showed an overall activity increase or decrease independent of stimulus identity, whereas 15 neurons (20%) fired differentially for the six sample stimuli and predicted the upcoming choice response. Incidentally, the prevalence of neurons preferring leftwards and rightwards responses was similar in both hemispheres.

Choice phase

The choice phase was defined as the time period starting from the 'confirmation' key peck that terminated illumination of the center key ('leaving time') to the first subsequent key peck registered at either of the two choice keys (see Fig. 1A). Figure 5A and B shows spike-density functions of two example neurons preferring rightwards and leftwards movement, respectively. These neurons started to differentiate movement directions after the animal left the center key (dotted vertical lines in Fig. 5a2 and b2) and continued to do so until the animal pecked at the respective choice key (time 0). Overall, 59/75 neurons (79%) showed significant activity changes during choice compared with spontaneous activity, with 27 neurons increasing and 32 neurons reducing activity ($P < 0.05$, Kruskal–Wallis test; Fig. 5C). Moreover, 30/75 neurons (40%) differentiated between leftwards and rightwards movements, with 20 neurons firing more for leftwards and 10 neurons firing more for rightwards movements ($P < 0.05$, Kruskal–Wallis test; Fig. 5D). Neurons preferring leftwards and rightwards responses were distributed roughly equally across the two hemispheres. Again, effect sizes were smoothly distributed, indicating no clear demarcated neural subclasses. Comparison of neural activity on correct and error trials in the manner conducted for the sample phase revealed significant differences between all conditions that entailed different choice directions (Wilcoxon signed-rank test, $P < 0.05$, $n = 21$), but no significant differences when choice directions were identical, regardless of whether these responses were correct or incorrect (Fig. 5E). This indicates that neural activity in this subsample of neurons solely represented motor activity without any information on either the luminance of the preceding stimulus or whether the currently executed choice was correct.

Outcome phase

The outcome phase was defined as the time period starting from the key peck registered at one of the two choice keys and ending with either the offset of the feeder light (correct trials, concurrent with the offset of the food hopper when food was delivered) or the offset of the time-out punishment interval (incorrect trials). Also, 66 out of the 75 neurons were tested with occasional free rewards delivered during the ITI; the same neurons were tested with a delay period between correct choice key response and reward delivery (see Materials and methods). This delay was introduced in order to more clearly separate the sensory and motor events of the choice phase and those of the outcome phase. Importantly, reward delivery became increasingly unlikely over time; the overall reward probability for correct choices was only 0.4, and the timing of reward delivery was deliberately left uncertain, occurring after 1, 2, or 3 s of waiting with probabilities of 0.5, 0.33, and 0.17, respectively. This manipulation was conducted in order to test whether NCL neural firing rates might convey a surprise signal or a reward prediction error, as hinted at previously (Kirsch *et al.*, 2009).

Figure 6A shows an example neuron firing vividly during reward presentation, regardless of whether the reward followed a correct choice (blue) or was given unexpectedly during the ITI (blue or green, respectively) (see Fig. 6a1 and a2). Following a correct

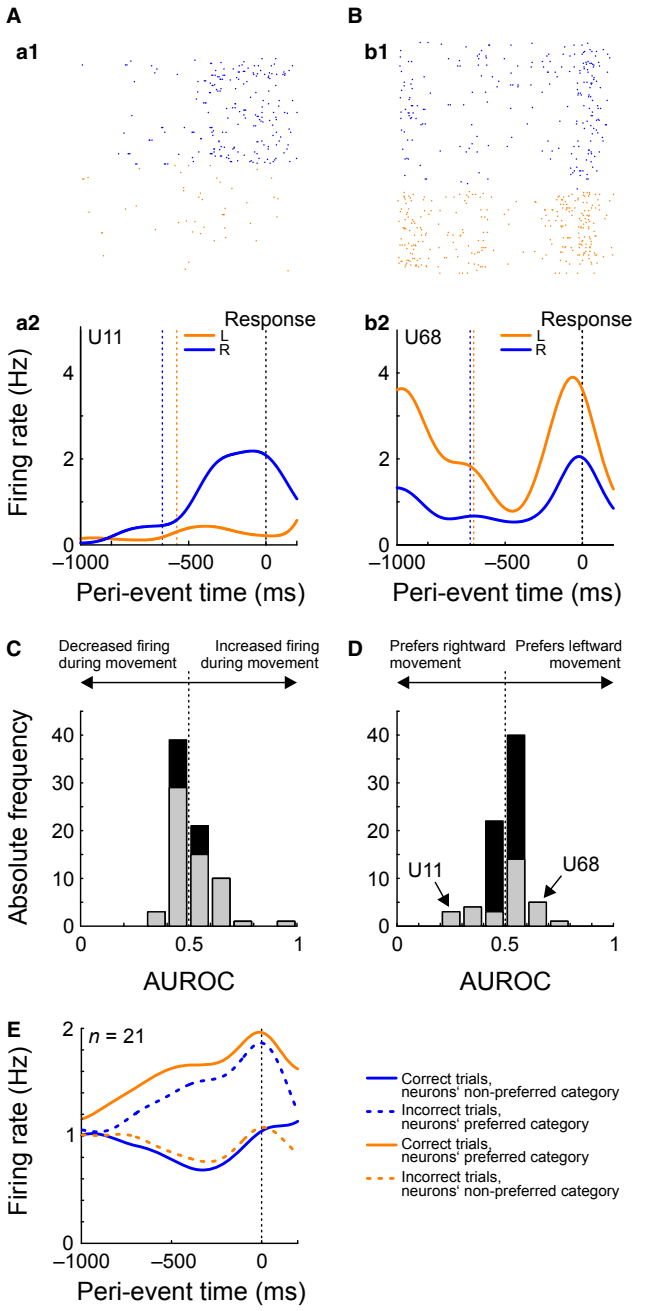

FIG. 5. Neural responses during the choice phase. (A) Spike-density functions (SDFs) of a neuron that responded during rightwards movements. Time 0 (black vertical dotted line) is the time at which the animal pecked at either choice key. Blue and orange dotted lines indicate median center key leaving times for rightwards and leftwards choices, respectively. (B) As in (A), but for a neuron that preferred leftwards movement. (C) Distribution of effect sizes (AUROC) for all neurons, comparing neural activity during a period of 400 ms before the choice key response with baseline activity. (D) As in (C), but comparing neural activity during leftwards and rightwards movements. (E) SDFs aligned to choice responses, split up according to whether movement direction was into the neurons' preferred or non-preferred direction, and whether the response was correct or not. Other conventions as in Fig. 2.

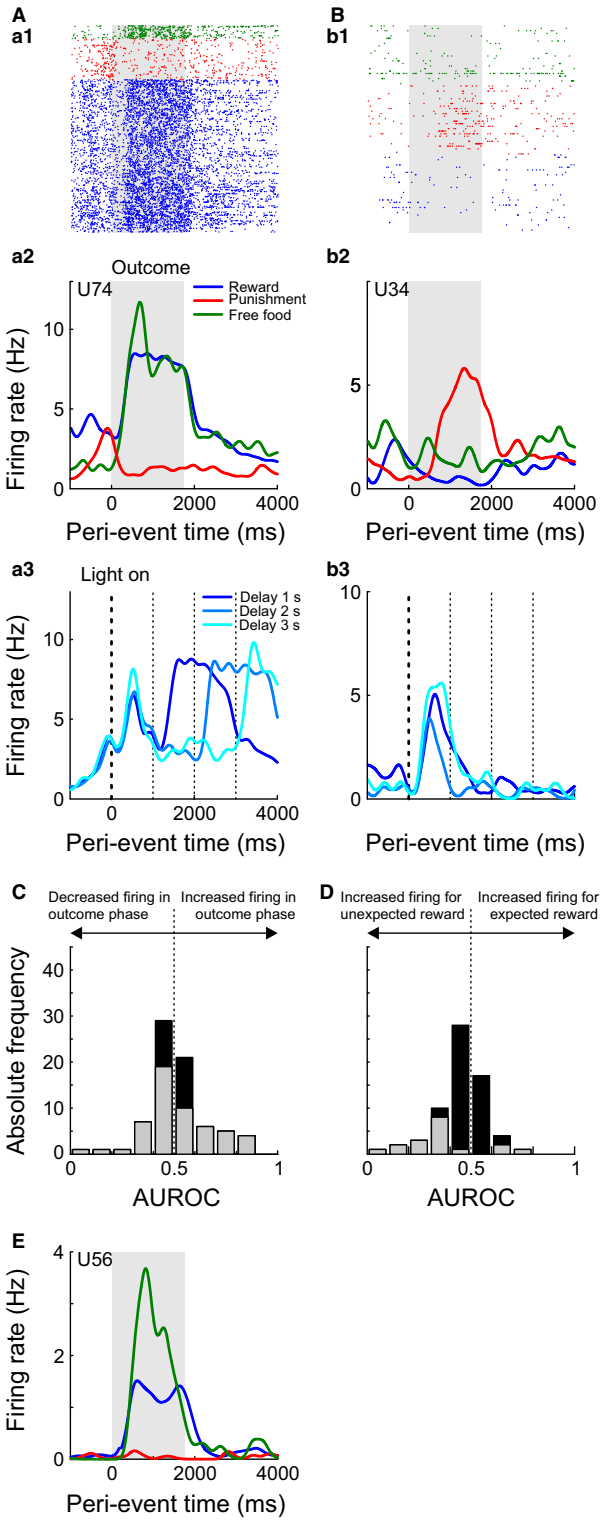

FIG. 6. Neural responses during the outcome phase. (A) Example neuron with elevated firing during reward presentation. (a1 and a2) Rasters and spike-density functions for reward, punishment, and free rewards (color-coded). (a3) Responses to reward aligned to the beginning of the outcome phase to illustrate activity during the delay phase. (B) As in (A), but showing results from a neuron with elevated responding to punishment. (C) Distribution of effect sizes (AUROC) for all neurons, comparing neural activity during the outcome phase (1.75 s of either reward or punishment) with baseline activity. (D) As in (C), but comparing neural activity during presentation of reward at the end of a correctly executed trial and unexpected reward occasionally presented between two trials. (E) As in (A), but showing results from a neuron firing more for unexpected than expected reward.

choice, the cell's activity peaked briefly when the feeder light was turned on, then declined and increased again immediately after food hopper activation (Fig. 6a3). However, this neuron's response pattern was not consistent with coding for a reward prediction error; free food was more unexpected than food at the end of the trials,

and food delivery became increasingly unlikely after 1, 2, and 3 s of waiting in the outcome phase, but still neural responses were no different in these cases.

The cell shown in Fig. 6B increased firing in response to time-out punishment (red in Fig. 6b1 and b2). Responding to reward was weak. Similar to the neuron in Fig. 6A, this cell's activity peaked shortly after feeder light onset, at the beginning of the delay period (Fig. 6b3).

In total, 54/75 (72%) neurons showed significant activity changes during the outcome phase, with 25 neurons increasing and 29 neurons decreasing activity relative to baseline firing ($P < 0.05$, Kruskal–Wallis test; Fig. 6C contrasting responses to both reward and punishment against spontaneous activity). Furthermore, 50/75 neurons (67%) were differentially modulated during the outcome phase, i.e. their activity differed between reward and punishment events (comparing spike counts within 0.1 s with 1.75 s after event onset). Comparison of firing rates during each outcome event with baseline firing revealed that, of 75 neurons, 58 changed firing during reward presentation (29 neurons increasing and 29 neurons decreasing activity), and 37 changed firing during punishment (27 increasing, 10 decreasing firing). Effect sizes (AUROC) were generally larger for reward than for punishment. Thus, NCL neurons were responsive to both kinds of choice outcomes tested in this study, but were more sensitive for reward presentation. Again, effect sizes were unimodally and continuously distributed (Fig. 6C and D).

Only 6/66 neurons (9%) differentiated between rewards delivered after different stimuli ($P < 0.05$, Kruskal–Wallis test), and only four of these reached moderately sized η^2 values (i.e. $0.1 < \eta^2 < 0.2$). In a similar vein, only 8/65 neurons showed graded firing during reward presentation after 1, 2, or 3 s of delay. Again, effect sizes were very small, with only one neuron exhibiting $\eta^2 > 0.1$. However, 18/66 (27%) neurons differentiated between free rewards and rewards delivered after correct choices, with 15 of those firing more for unexpected rewards (see distribution of effect sizes in Fig. 6D and example neuron in Fig. 6E), consistent with the notion that NCL neurons signal a positive reward prediction error as found in monkey lateral PFC (Asaad & Eskandar, 2011) or a surprise signal as in the anterior cingulate cortex (Roesch *et al.*, 2012).

Correlation of neural response properties across task phases

So far, we have discussed neural response patterns separately for each phase of the behavioral task. In this section, we will more closely examine the neural response patterns across all task phases for the three most prominent types of responses that we encountered: (i) unspecific modulation in the sample phase, (ii) stimulus-specific modulation in the sample phase, and (iii) reward modulation in the outcome phase.

Unspecific modulation in the sample phase

As detailed above, 80% of all neurons significantly changed their activity during key pecking in the sample phase, with the majority of neurons decreasing firing (see Fig. 2). As most of these neurons (60% of the total sample; henceforth dubbed peck-activation and peck-suppression units) did not fire differentially for the sample stimuli, it is tempting to speculate that they were involved in sensorimotor processes associated with key pecking. Because pecking to the response key is similar to pecking to consume the reward (Jenkins & Moore, 1973; Allan & Zeigler, 1994), it would be expected that many neurons would show the same behavior in both task phases (either increasing or decreasing their activity in both the sample and reward phases). Indeed, this is what we observed; there were positive correlations both between the AUROC values for the sample phase (Fig. 2C) and the AUROC values for (i) reward presentation ($r = 0.31$, $P < 0.01$, $n = 75$) and also (ii) choice response execution (Fig. 5C; $r = 0.52$, $P < 0.01$, $n = 75$). Put differently, peck-activation units tended to increase firing both during choice movements and during feeding, and the converse pattern held for peck-suppression units. This finding is consistent with the notion that many NCL neurons are involved in sensorimotor processing during response execution.

Differential activity modulation during sample presentation

Perhaps the most interesting NCL response profile is that shown in Fig. 3 because these neurons did not only differentiate between sample stimuli, but did so even well after the sample stimuli had been turned off, precluding the interpretation that these neurons were driven purely by sensory input. Indeed, 12 of the 15 neurons with significant differential modulation also showed significant modulation during the choice phase, and 7/15 neurons differentiated significantly between movement directions. Importantly, AUROC values for the distributions of spike counts for category C1 vs. C2 during the sample phase were positively correlated with the AUROC values in the choice phase, i.e. neurons firing more for category C1 stimuli (dark, requiring responding to the right choice key) also tended to fire more during rightwards motion in the choice phase, and vice versa ($r = 0.56$, $P = 0.03$, $n = 15$).

Reward modulation

Probably the most frequently found type of NCL neural response is that of either strong activation or suppression during reward presentation (Kalt *et al.*, 1999; Kirsch *et al.*, 2009; Koenen *et al.*, 2013; Starosta *et al.*, 2013). Indeed, 58/75 neurons in our sample significantly changed their activity during reward presentation. As noted in the previous section, it could be that this modulation of activity is related to sensorimotor events accompanying reward consumption, such as the individual pecking movements towards the grain kernels. As the pecking movements associated with grain consumption are comparable to those emitted towards a visual stimulus predicting food reinforcement (see above), we asked whether the degree of modulation by reward relative to baseline firing was correlated with key pecking during the sample phase. Indeed, 48/58 reward neurons were modulated during the sample phase relative to baseline firing, and the correlation between the AUROC effect sizes for the sample phase and reward presentation was 0.31 (same analysis as in previous section). Taken together, these results indicate that neural activity changes during reward were partly due to sensorimotor features associated with pecking movements.

Histology

Figure 7 shows coronal slices of the pigeon brain adapted from the stereotaxic atlas of Karten & Hodos (1967), with estimated positions of the electrode tracks superimposed. The brain of one animal (bird 919) was damaged during extraction, and electrode tracks could not be recovered with certainty. For all other birds, the cannula tracks were found to be situated within the borders of the NCL as defined by Herold *et al.* (2011).

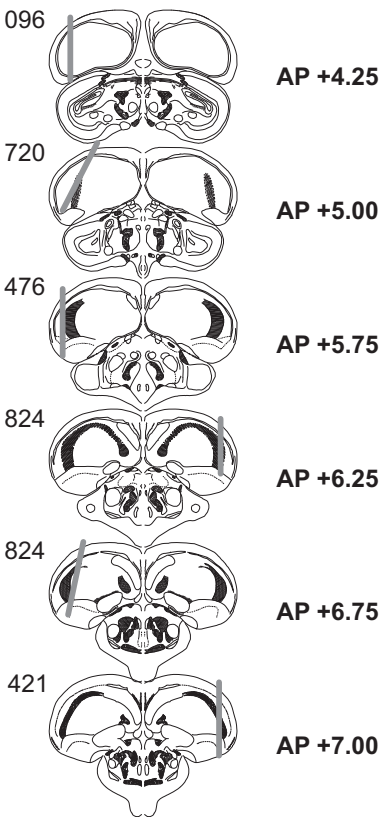

FIG. 7. Histology. Coronal slices from the stereotaxic atlas by Karten & Hodos (1967). Gray lines indicate estimated electrode tracks. AP, anterior–posterior axis.

Discussion

As hypothesised on the basis of previous findings, we found that the NCL is involved in perceptual decision making, as demonstrated by the modulation of neural firing rates across all phases of the psychophysical task. Whereas many neurons unspecifically increased or decreased firing during stimulus presentation, a subset of neurons fired differentially for the sample stimuli and signaled the upcoming choice response. In addition, most NCL neurons responded to reward delivery, and several of these fired more for unexpected than expected reward. In the following, we will discuss these findings one by one.

Sensorimotor-related activity

Whereas studies in head-fixed pigeons found only very few neurons with motor-related response modulation (Kalt *et al.*, 1999; Kirsch *et al.*, 2009), the present study and another recent study with freely moving pigeons (Starosta *et al.*, 2013) suggest that a much larger fraction of NCL neurons is involved in sensorimotor processing than previously thought. One explanation for the paucity of sensorimotor-related activity found in head-fixed preparations may be the limited range of movements that subjects could execute in that situation (using beak openings as operant responses). It is striking that peck-activation and peck-suppression units (descriptive labels taken to highlight that these neurons changed firing during sample presentation irrespective of the stimulus identity) made up 60% of our total sample. In addition, these neurons responded similarly during key pecking and reward consumption, and it has been shown that conditioned pecking to visual stimuli predicting food is similar to pecking to the food itself (Brown & Jenkins, 1968; Allan & Zeigler, 1994). Accordingly, these two types of neurons could represent sensorimotor aspects of pecking movements – either part of the motor command for key pecking or kinesthetic (trigeminal) feedback (Bermejo & Zeigler, 1999).

Alternatively, peck-activation and peck-suppression neurons could represent specific actions that are executed or inhibited, respectively. We frequently observed phasic activity peaks following the registration of the choice response, i.e. during a delay period that intervened between choice and subsequent reward delivery (see Fig. 6A and B for examples). Neurons in the macaque PFC exhibit similar activity peaks signifying the end of a sequence of saccadic eye movements (Fujii & Graybiel, 2003). Indeed, transient inactivation of the NCL results in circumscribed deficits in the initiation and execution of cue-guided action sequences (Helduser & Güntürkün, 2012), raising the interesting possibility that the peaks that we observed represent a similar signal.

Differential activity in the sample phase

The neurons whose responses were differentially modulated by the stimuli showed nearly monotonic increases or decreases in firing rate as a function of stimulus luminance. Additional analyses revealed that these activity patterns were predictive of the response direction in the subsequent choice phase. Thus, these neurons seem to convey a motor plan for the execution of leftwards or rightwards head movements, rather than representing stimulus luminance. The interpretation that these neurons are involved in action planning resonates well with several previous results: (i) temporary blockade of *N*-methyl-D-aspartate receptors in the NCL results in impaired response selection in matching-to-sample tasks (Lissek & Güntürkün, 2004, 2005), (ii) transient inactivation of the NCL through tetrodotoxin leads to an overall suppression of operant behavior (Lengersdorf *et al.*, 2014) and (iii) impairs the execution of learned action sequences, leading to both action omission and action perseveration without impairment of visuomotor performance (Helduser & Güntürkün, 2012).

At the same time, the NCL response patterns during the sample phase resembled those found in the lateral intraparietal and dorsolateral PFC of monkeys in saccadic choice tasks (see Figs 3 and 4; compare, e.g. with Kim & Shadlen, 1999; Shadlen & Newsome, 2001). In both the NCL and cortex, neural firing rates ramp up during stimulus presentation and then stay at a constant level until a choice response is initiated. Importantly, the slope of the firing rate increase is determined by the difficulty of the decision, being steep for easy and shallow for difficult sample stimuli. Such response patterns are predicted by a class of sequential-sampling models (Smith & Ratcliff, 2004). Put simply, these models assume that, during stimulus presentation, noisy sensory information ('evidence') is integrated over time until sufficient evidence has accumulated to determine which of several possible stimulus classes is presented; at that time, an appropriate choice response is initiated. The trajectory of evidence integration posited by these models bears close resemblance to the patterns of neural firing in the cortex of non-human primates performing visual discrimination tasks (Gold & Shadlen, 2007). To our knowledge, this study is the first to demonstrate similar neural response patterns in a species other than monkeys, testifying to the power and generality of these models across different species. Accordingly, it will be important to further explore the degree to which NCL neural firing rates reflect evidence accumulation for a particular action, e.g. by employing reaction-time tasks and microstimulation (Hanks *et al.*, 2006).

Reward coding

Our task included systematic manipulations of subjective reward probability during the outcome phase, which enabled us to test whether NCL neurons signal a reward prediction error or surprise signal as found, for example, in monkey dorsolateral prefrontal and anterior cingulate cortex, respectively (Asaad & Eskandar, 2011; Roesch *et al.*, 2012). Although very few neurons (9%) differentiated between rewards delivered at different time points with different probabilities, we found that 18/66 (27%) neurons fired differentially for expected and unexpected reward, with the majority of neurons (15) firing more for unexpected rewards. This suggests that NCL neurons do not bluntly respond to reward delivery but may represent more elaborate reward properties, such as the degree to which its occurrence was expected, which constitutes an important factor in animal learning theory (Rescorla & Wagner, 1972).

Comparing the nidopallium caudolaterale and prefrontal cortex at the single-neuron level

We have highlighted several phenomenological similarities of NCL and PFC single-neuron response profiles. Above and beyond these findings, there exist further parallels of NCL and orbitofrontal cortex response patterns in a very similar paradigm employing rats (Feierstein *et al.*, 2006). First, a minor fraction of neurons (~20%) in both structures predicted choice direction before choice initiation; second, a major fraction of neurons (~70%) was modulated during the outcome period; and third, more neurons increased firing for negative outcomes [orbitofrontal cortex, reward omission; NCL, reward omission, punishment; also see Starosta *et al.* (2013)] than for positive outcomes (reward presentation).

Comparative research involving non-mammalian species is conducted mostly at the levels of gross neuroanatomy, cytoarchitectonics, and connectivity (Striedter *et al.*, 2014). There exists very little research comparing the implementation of particular behavioral functions at the level of single-neuron spiking activity. Moreover, investigations of the response properties of single neurons during behavioral performance in amphibians, reptiles and fish are virtually non-existent, and such data are sparse even for birds. In the case of the NCL, available evidence suggests an astonishing degree of phenomenological similarity to the PFC at the single-neuron level (Diekamp *et al.*, 2002b; Veit & Nieder, 2013; present study), even though these structures are not homologous and are very different in terms of cytoarchitectonics (nuclear vs. layered, respectively). Although an earlier study from our laboratory suggests a subdivision between the ventral and dorsal NCL (Diekamp *et al.*, 2002b), it is not known whether these or any other subdivisions of the NCL correspond to subdivisions of the PFC. Also, we did not find any obvious segregation of neural response properties. Importantly, the NCL and PFC are neither homologous nor similar in terms of their neural architecture but seem to constitute a case of evolutionary convergence (Güntürkün, 2012), so there is no particular reason to assume that any subdivisions of the mammalian PFC map correspond one-to-one to subdivisions of the avian NCL.

The picture of the NCL emerging from this study is that of a structure concerned with response selection and response execution. Moreover, our data show that the notion of functional equivalence of the NCL and PFC, up to now based largely on lesion studies (but see Diekamp *et al.*, 2002b), extends to the level of single-neuron response profiles. Disentangling the contributions of sensorimotor and cognitive variables to NCL neural responses will be crucial to further constrain hypotheses on the precise function of this structure as well as its relation to subdivisions of the mammalian PFC (Wise, 2008; Herold *et al.*, 2011).

Acknowledgements

This research was supported by grants from the German Research Foundation to M.C.S. (DFG STU 544/1-1) and O.G. (DFG SFB 874).

Abbreviations

AUROC, area under the receiver operating characteristic curve; ITI, intertrial interval; NCL, nidopallium caudolaterale; PFC, prefrontal cortex; PI, predictive index; PPTH, peri-peck time histogram.

Author contributions

M.C.S. and O.G. conceived the research. D.L., M.C.S. and R.P. performed the experiments. D.L. and M.C.S. analysed the data. M.C.S. wrote the paper.

References

Allan, R.W. & Zeigler, H.P. (1994) Autoshaping the pigeon's gape response: acquisition and topography as a function of reinforcer type and magnitude. *J. Exp. Anal. Behav.*, **62**, 201–223.

Alsop, B. (1998) Receiver operating characteristics from nonhuman animals: some implications and directions for research with humans. *Psychon. B. Rev.*, **5**, 239–252.

Asaad, W.F. & Eskandar, E.N. (2011) Encoding of both positive and negative reward prediction errors by neurons of the primate lateral prefrontal cortex and caudate nucleus. *J. Neurosci.*, **31**, 17772–17787.

Bermejo, R. & Zeigler, H.P. (1999) Trigeminal deafferentation and conditioned pecking in pigeons. *Behav. Brain Res.*, **99**, 181–189.

Bilkey, D.K. & Muir, G.M. (1999) A low cost, high precision subminiature microdrive for extracellular unit recording in behaving animals. *J. Neurosci. Meth.*, **92**, 87–90.

Bilkey, D.K., Russell, N. & Colombo, M. (2003) A lightweight microdrive for single-unit recording in freely moving rats and pigeons. *Methods*, **30**, 152–158.

Blough, D.S. (1963) Interresponse time as a function of continuous variables: a new method and some data. *J. Exp. Anal. Behav.*, **6**, 237–246.

Boneau, C.A. & Cole, J.L. (1967) Decision theory, the pigeon, and the psychophysical function. *Psychol. Rev.*, **74**, 123–135.

Brown, P. & Jenkins, H. (1968) Autoshaping of the pigeon's key-peck. *J. Exp. Anal. Behav.*, **11**, 1–8.

Browning, R., Overmier, J.B. & Colombo, M. (2011) Delay activity in avian prefrontal cortex–sample code or reward code? *Eur. J. Neurosci.*, **33**, 726–735.

Brunton, B., Botvinick, M. & Brody, C. (2013) Rats and humans can optimally accumulate evidence for decision-making. *Science*, **340**, 95–98.

Cohen, J. (1992) A power primer. *Psychol. Bull.*, **112**, 155–159.

De Lafuente, V. & Romo, R. (2005) Neuronal correlates of subjective sensory experience. *Nat. Neurosci.*, **8**, 1698–1703.

Diekamp, B., Gagliardo, A. & Güntürkün, O. (2002a) Nonspatial and subdivision-specific working memory deficits after selective lesions of the avian prefrontal cortex. *J. Neurosci.*, **22**, 9573–9580.

Diekamp, B., Kalt, T. & Güntürkün, O. (2002b) Working memory neurons in pigeons. *J. Neurosci.*, **22**, RC210.

Feierstein, C.E., Quirk, M.C., Uchida, N., Sosulski, D.L. & Mainen, Z.F. (2006) Representation of spatial goals in rat orbitofrontal cortex. *Neuron*, **51**, 495–507.

Fujii, N. & Graybiel, A. (2003) Representation of action sequence boundaries by macaque prefrontal cortical neurons. *Science*, **301**, 1246–1249.

Fuster, J.M. (1973) Unit activity in prefrontal cortex during delayed-response performance: neuronal correlates of transient memory. *J. Neurophysiol.*, **36**, 61–78.

Gold, J.I. & Shadlen, M.N. (2002) Banburismus and the brain: decoding the relationship between sensory stimuli, decisions, and reward. *Neuron*, **36**, 299–308.

Gold, J.I. & Shadlen, M.N. (2007) The neural basis of decision making. *Annu. Rev. Neurosci.*, **30**, 535–574.

Goodale, M.A. (1983) Visually guided pecking in the pigeon (*Columba livia*). *Brain Behav. Evolut.*, **22**, 22–41.
Green, D.M. & Swets, J.A. (1988) *Signal Detection Theory and Psychophysics*. Peninsula Publishing, Los Altos Hills.
Güntürkün, O. (1997) Cognitive impairments after lesions of the neostriatum caudolaterale and its thalamic afferent in pigeons: functional similarities to the mammalian prefrontal system? *J. Hirnforsch.*, **38**, 133–143.
Güntürkün, O. (2005) The avian "prefrontal cortex" and cognition. *Curr. Opin. Neurobiol.*, **15**, 686–693.
Güntürkün, O. (2012) The convergent evolution of neural substrates for cognition. *Psychol. Res.*, **76**, 212–219.
Hanks, T.D., Ditterich, J. & Shadlen, M.N. (2006) Microstimulation of macaque area LIP affects decision-making in a motion discrimination task. *Nat. Neurosci.*, **9**, 682–689.
Hartmann, B. & Güntürkün, O. (1998) Selective deficits in reversal learning after neostriatum caudolaterale lesions in pigeons: possible behavioral equivalencies to the mammalian prefrontal system. *Behav. Brain Res.*, **96**, 125–133.
Helduser, S. & Güntürkün, O. (2012) Neural substrates for serial reaction time tasks in pigeons. *Behav. Brain Res.*, **230**, 132–143.
Hentschke, H. & Stüttgen, M.C. (2011) Computation of measures of effect size for neuroscience data sets. *Eur. J. Neurosci.*, **34**, 1887–1894.
Herold, C., Palomero-Gallagher, N., Hellmann, B., Kröner, S., Theiss, C., Güntürkün, O. & Zilles, K. (2011) The receptor architecture of the pigeons' nidopallium caudolaterale: an avian analogue to the mammalian prefrontal cortex. *Brain Struct. Funct.*, **216**, 239–254.
Jenkins, H.M. & Moore, B.R. (1973) The form of the auto-shaped response with food or water reinforcers. *J. Exp. Anal. Behav.*, **20**, 163–181.
Kalt, T., Diekamp, B. & Güntürkün, O. (1999) Single unit activity during a Go/NoGo task in the "prefrontal cortex" of pigeons. *Brain Res.*, **839**, 263–278.
Karten, H.J. & Hodos, W. (1967) *A Stereotaxic Atlas of the Brain of the Pigeon (Columba livia)*. Johns Hopkins Press, Baltimore.
Kim, J.N. & Shadlen, M.N. (1999) Neural correlates of a decision in the dorsolateral prefrontal cortex of the macaque. *Nat. Neurosci.*, **2**, 176–185.
Kirsch, J.A., Vlachos, I., Hausmann, M., Rose, J., Yim, M.Y., Aertsen, A. & Güntürkün, O. (2009) Neuronal encoding of meaning: establishing category-selective response patterns in the avian "prefrontal cortex". *Behav. Brain Res.*, **198**, 214–223.
Koenen, C., Millar, J. & Colombo, M. (2013) How bad do you want it? Reward modulation in the avian nidopallium caudolaterale. *Behav. Neurosci.*, **127**, 544–554.
Krupa, D.J., Matell, M.S., Brisben, A.J., Oliveira, L.M. & Nicolelis, M.A.L. (2001) Behavioral properties of the trigeminal somatosensory system in rats performing whisker-dependent tactile discriminations. *J. Neurosci.*, **21**, 5752–5763.
Lengersdorf, D., Stüttgen, M.C., Uengoer, M. & Güntürkün, O. (2014) Transient inactivation of the pigeon hippocampus or the nidopallium caudolaterale during extinction learning impairs extinction retrieval in an appetitive conditioning paradigm. *Behav. Brain Res.*, **265**, 93–100.
Lissek, S. & Güntürkün, O. (2004) Maintenance in working memory or response selection? Functions of NMDA receptors in the pigeon "prefrontal cortex". *Behav. Brain Res.*, **153**, 497–506.
Lissek, S. & Güntürkün, O. (2005) Out of context: NMDA receptor antagonism in the avian "prefrontal cortex" impairs context processing in a conditional discrimination task. *Behav. Neurosci.*, **119**, 797–805.
Mogensen, J. & Divac, I. (1982) The prefrontal "cortex" in the pigeon. Behavioral evidence. *Brain Behav. Evolut.*, **21**, 60–66.
Mogensen, J. & Divac, I. (1993) Behavioural effects of ablation of the pigeon-equivalent of the mammalian prefrontal cortex. *Behav. Brain Res.*, **55**, 101–107.
Newsome, W.T., Britten, K.H. & Movshon, J.A. (1989) Neuronal correlates of a perceptual decision. *Nature*, **341**, 52–54.
Reiner, A., Yamamoto, K. & Karten, H.J. (2005) Organization and evolution of the avian forebrain. *Anat. Rec. Part A.*, **287**, 1080–1102.
Rescorla, R.A. & Wagner, A.R. (1972) A theory of Pavlovian conditioning: variations in the effectiveness of reinforcement and nonreinforcement. In Black, A.H. & Prokasy, W.F. (Eds), *Classical Conditioning II: Current Research and Theory*. Appleton-Century-Crofts, New York, pp. 64–99.
Roesch, M.R., Esber, G.R., Li, J., Daw, N.D. & Schoenbaum, G. (2012) Surprise! Neural correlates of Pearce-Hall and Rescorla-Wagner coexist within the brain. *Eur. J. Neurosci.*, **35**, 1190–1200.
Rose, J., Otto, T. & Dittrich, L. (2008) The Biopsychology-Toolbox: a free, open-source Matlab-toolbox for the control of behavioral experiments. *J. Neurosci. Meth.*, **175**, 104–107.
Shadlen, M.N. & Newsome, W.T. (2001) Neural basis of a perceptual decision in the parietal cortex (area LIP) of the rhesus monkey. *J. Neurophysiol.*, **86**, 1916–1936.
Smith, P.L. & Ratcliff, R. (2004) Psychology and neurobiology of simple decisions. *Trends Neurosci.*, **27**, 161–168.
Starosta, S., Güntürkün, O. & Stüttgen, M.C. (2013) Stimulus-response-outcome coding in the pigeon nidopallium caudolaterale. *PLoS One*, **8**, e57407.
Starosta, S., Stüttgen, M.C. & Güntürkün, O. (2014) Recording single neurons' action potentials in freely moving pigeons across three stages of learning. *J. Vis. Exp.*, **88**, e51283.
Striedter, G.F. (2013) Bird brains and tool use: beyond instrumental conditioning. *Brain Behav. Evolut.*, **82**, 55–67.
Striedter, G.F., Belgard, T.G., Chen, C.-C., Davis, F.P., Finlay, B.L., Güntürkün, O., Hale, M.E., Harris, J.A., Hecht, E.E., Hof, P.R., Hofmann, H.A., Holland, L.Z., Iwaniuk, A.N., Jarvis, E.D., Karten, H.J., Katz, P.S., Kristan, W.B., Macagno, E.R., Mitra, P.P., Moroz, L.L., Preuss, T.M., Ragsdale, C.W., Sherwood, C.C., Stevens, C.F., Stüttgen, M.C., Tsumoto, T. & Wilcynski, W. (2014) NSF workshop report: discovering general principles of nervous system organization by comparing brain maps across species. *J. Comp. Neurol.*, **522**, 1445–1453.
Stüttgen, M.C., Schwarz, C. & Jäkel, F. (2011a) Mapping spikes to sensations. *Front. Neurosci.*, **5**, 125.
Stüttgen, M.C., Yildiz, A. & Güntürkün, O. (2011b) Adaptive criterion setting in perceptual decision making. *J. Exp. Anal. Behav.*, **96**, 155–176.
Stüttgen, M.C., Kasties, N., Lengersdorf, D., Starosta, S., Güntürkün, O. & Jäkel, F. (2013) Suboptimal criterion setting in a perceptual choice task with asymmetric reinforcement. *Behav. Process.*, **96**, 59–70.
Thorpe, S.J., Rolls, E.T. & Maddison, S. (1983) The orbitofrontal cortex – neuronal-activity in the behaving monkey. *Exp. Brain Res.*, **49**, 93–115.
Veit, L. & Nieder, A. (2013) Abstract rule neurons in the endbrain support intelligent behaviour in corvid songbirds. *Nat. Commun.*, **4**, 2878.
Wise, S.P. (2008) Forward frontal fields: phylogeny and fundamental function. *Trends Neurosci.*, **31**, 599–608.
Zariwala, H.A., Kepecs, A., Uchida, N., Hirokawa, J. & Mainen, Z.F. (2013) The limits of deliberation in a perceptual decision task. *Neuron*, **78**, 339–351.
Zeigler, H.P., Levitt, P.W. & Levine, R.R. (1980) Eating in the pigeon (*Columba livia*): movement patterns, stereotypy, and stimulus control. *J. Comp. Physiol. Psych.*, **94**, 783–794.